Supplementary Information

Generalized high-temperature synthesis of zeolite catalysts with unpredictably high space-time yields (STYs)

Chaoqun Bian,[a] Changsheng Zhang,[a] Shuxiang Pan,[a] Fang Chen,[a] Weiping Zhang,[b] Xiangju Meng,*[,a] Stefan Maurer,[c] Daniel Dai,[c] Andrei-Nicolae Parvulescu,[d] Ulrich Müller,[d] and Feng-Shou Xiao.*[,a]

[a] Key Lab of Applied Chemistry of Zhejiang Province, Department of Chemistry, Zhejiang University, Hangzhou 310007, China.

[b] State Key Laboratory of Fine Chemicals, Dalian University of Technology, Linggong Road 2, Dalian 116024, China.

[c] BASF Catalysts (Shanghai) Co., Ltd., 239 Luqiao Road, Jinqiao Export Process Zone Pudong New District, Shanghai, 201206 , China.

[d] BASF SE, GCC/PZ - M311, 67056 Ludwigshafen, Germany.

Table S1 Textural parameters of various zeolites from hydrothermal routes

Sample	BET Area [a] m^2/g	Micropore Volume [a] cm^3/g
C-MFI	360	0.16
C-MOR	401	0.19
C-Beta	460	0.20
C-RUB-36	300	0.13

[a] The data were measured with H-form of zeolites synthesized from hydrothermal routes.

Table S2 RUB-36 zeolites synthesized from solvent-free and hydrothermal routes

Run	DMDEA/Si	Temperature (°C)	Time (day)	Zeolite type
1	0.07	140	20	RUB-36
2	0.07	160	9	RUB-36
3	0.07	180	3	RUB-36
4	0.07	200	1.5	RUB-36
5	0.43	140	14	RUB-36
6	0.43	160	9	Amor
7	0.43	180	3	Amor
8	0.43	200	2	Amor

Supplementary Figure Captions

Fig. S1 XRD patterns of the S-RUB-36-temp synthesized at (a) 140 °C for 20 days, (b) 160 °C for 9 days, (c) 180 °C for 3 days, and (d) 200 °C for 1.5 days.

Fig. S2 (a) XRD pattern and (b) SEM image of the C-RUB-36-140.

Fig. S3 TG curves of the (a) C-RUB-36-140, (b) S-RUB-36-140, and (c) S-RUB-36-180.

Fig. S4 ^{29}Si MAS NMR spectra of the (a) C-RUB-36, (b) S-RUB-36-140, and (c) S-RUB-36-180.

Fig. S5 XRD patterns of the S-RUB-36-180 crystallized at (a) 0, (b) 0.25, (c) 0.5, (d) 1.0, (e) 3.0, and (f) 4.0 days, respectively.

Fig. S6 SEM images of the S-RUB-36-180 crystallized at (a) 0, (b) 0.25, (c) 0.5, (d) 1.0, (e) 3.0, and (f) 4.0 days, respectively.

Fig. S7 Photographs of the S-RUB-36-180 crystallized at (a) 0, (b) 0.5, (c) 1.0, and (d) 4.0 days, respectively.

Fig. S8 ^{29}Si MAS NMR spectra of the S-RUB-36-180 crystallized at (a) 0, (b) 1.0, and (c) 4.0 days, respectively.

Fig. S9 XRD patterns of the S-RUB-36-140 crystallized at (a) 0, (b) 10, (c) 15, (d) 20, and (e) 25 days, respectively.

Fig. S10 The dependences of crystallinity on the crystallization time of the (a) C-RUB-36-140, (b) S-RUB-36-140, and (c) S-RUB-36-180.

Fig. S11 (A) SEM images and (B) XRD patterns of the (a) Beta seeds, (b) MFI seeds, and (c) MOR seeds.

Fig. S12 (A) SEM images and (B) XRD patterns of the S-Beta-200 crystallized at (a) 0, (b) 0.5, (c) 1, (d) 1.5, (e) 4, and (f) 5 h, respectively. There is impurity of MOR zeolite when the crystallization time reaches to 5 h.

Fig. S13 (A) SEM images and (B) XRD patterns of the S-MFI-240 crystallized at (a) 0, (b) 0.35, and (c) 0.5 h, respectively.

Fig. S14 (A) SEM images and (B) XRD patterns of the S-MOR-240 crystallized at (a) 0, (b) 1, and (c) 1.5 h, respectively.

Fig. S15 Catalytic conversion and product selectivities over S-ZSM-5-240 catalyst in MTO (■ C_1; ▲C_{2-4}; ▼$C_2^=$; ◄$C_3^=$;◆$C_4^=$; 🕓C_5+ aromatics; ►Conv.).

Fig. S16 Catalytic conversion and product selectivities over ZSM-5 catalyst by hydrothermal method at 180 °C in MTO (■ C_1; ▲C_{2-4}; ▼$C_2^=$; ◄$C_3^=$;◆$C_4^=$; 🕓C_5+ aromatics; ►Conv., the Si/Al ratio is 128 measured by ICP)

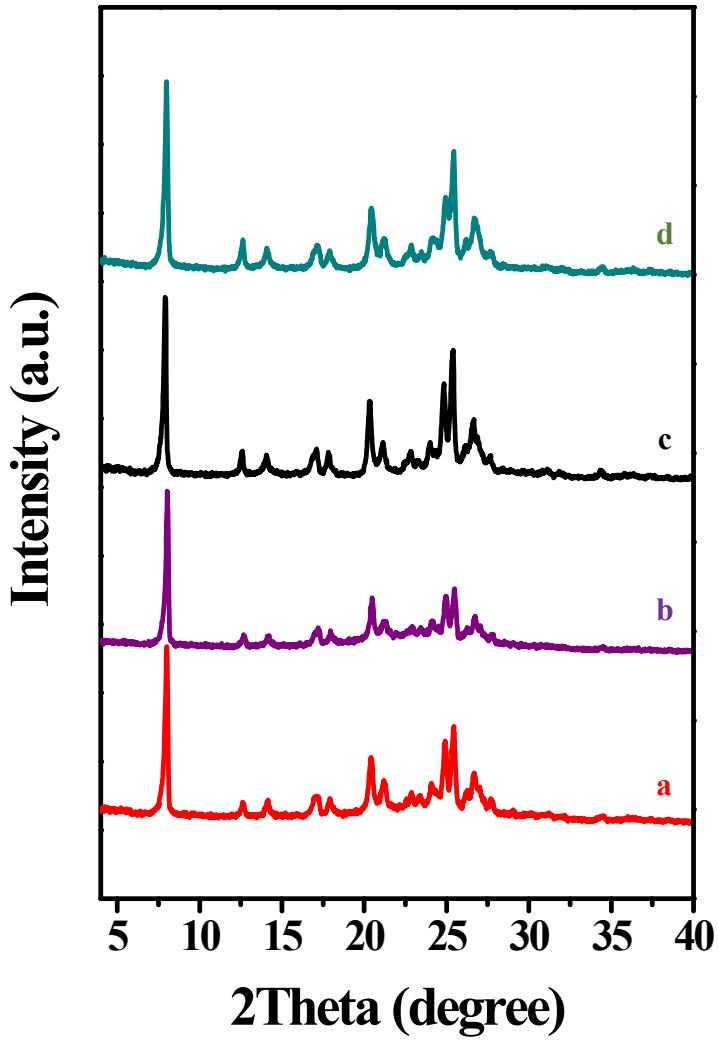

Fig. S1 XRD patterns of the S-RUB-36-temp synthesized at (a) 140 °C for 20 days, (b) 160 °C for 9 days, (c) 180 °C for 3 days, and (d) 200 °C for 1.5 days.

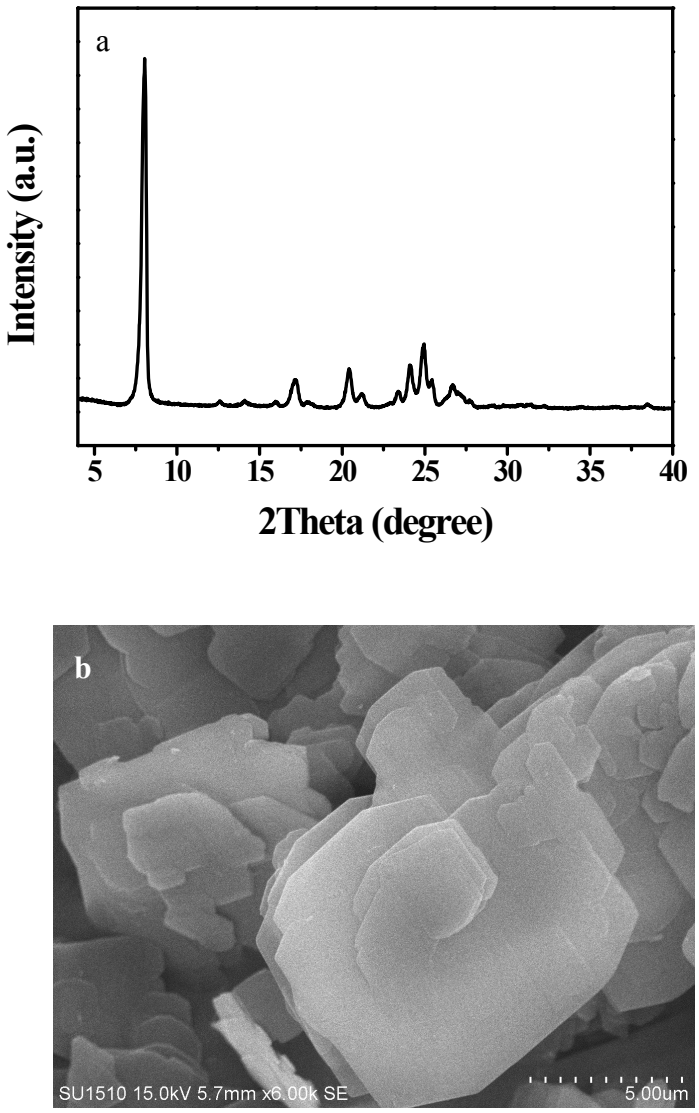

Fig. S2 (a) XRD pattern and (b) SEM image of the C-RUB-36-140.

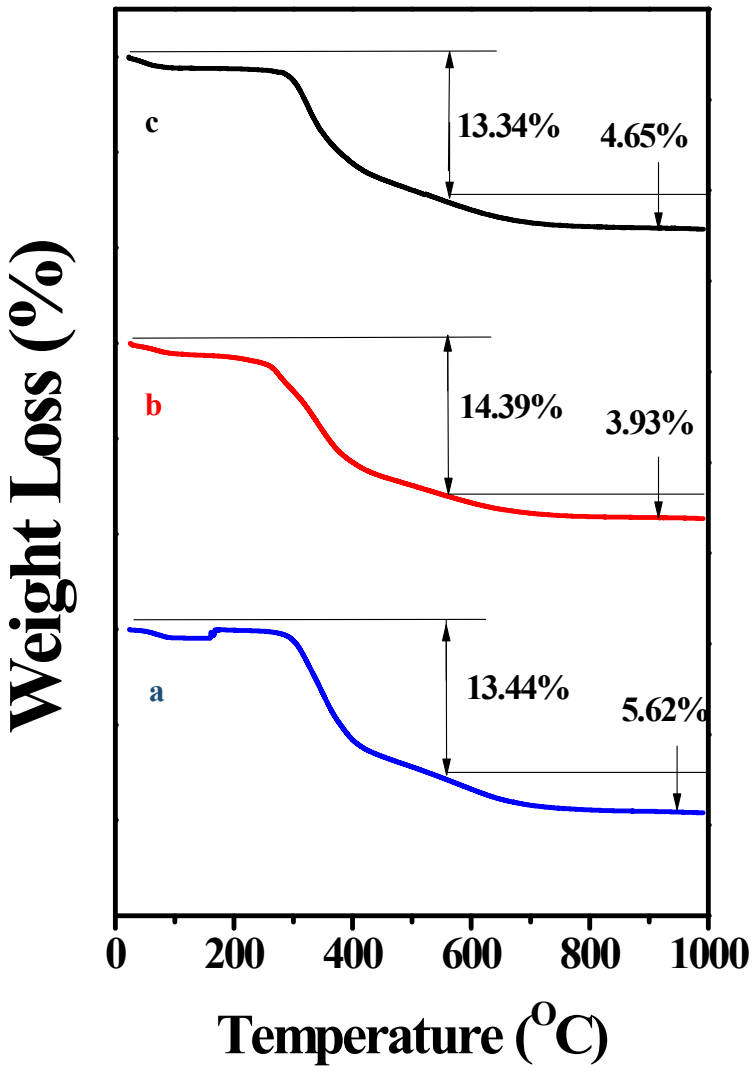

Fig. S3 TG curves of the (a) C-RUB-36-140, (b) S-RUB-36-140, and (c) S-RUB-36-180.

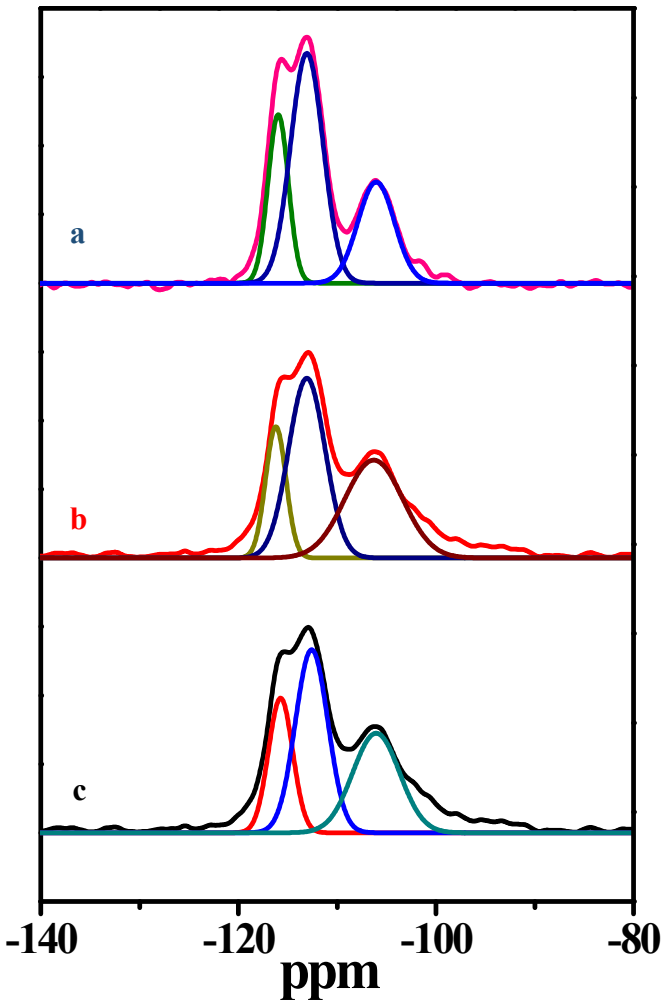

Fig. S4 ^{29}Si MAS NMR spectra of the (a) C-RUB-36-140, (b) S-RUB-36-140, and (c) S-RUB-36-180.

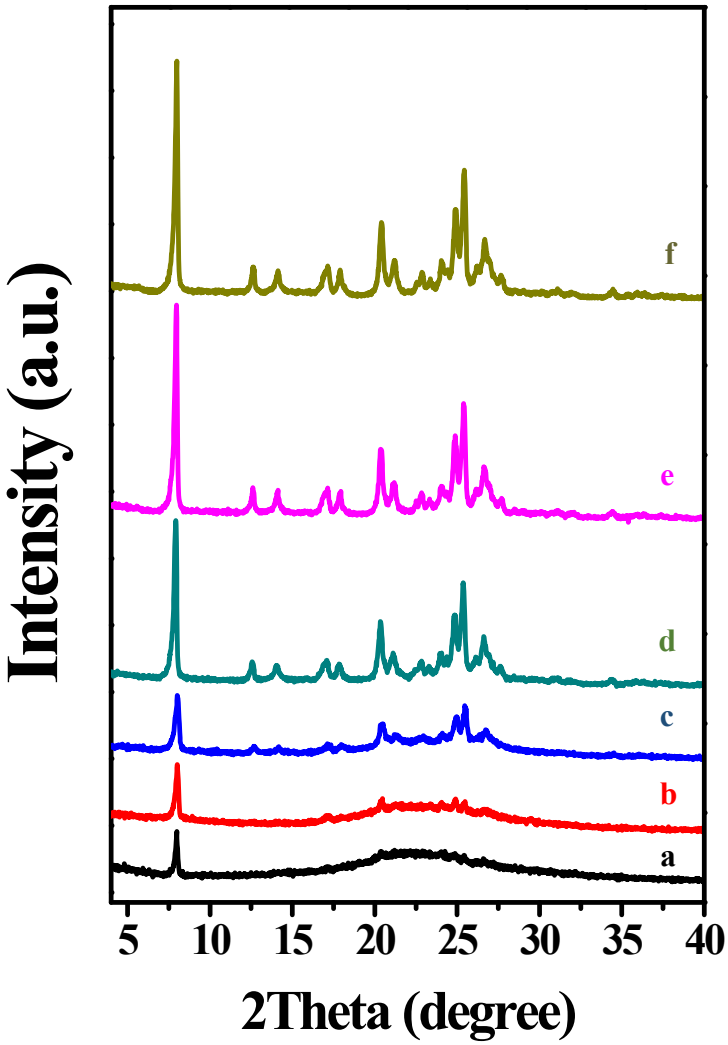

Fig. S5 XRD patterns of the S-RUB-36-180 crystallized at (a) 0, (b) 0.25, (c) 0.5, (d) 1.0, (e) 3.0, and (f) 4.0 days, respectively.

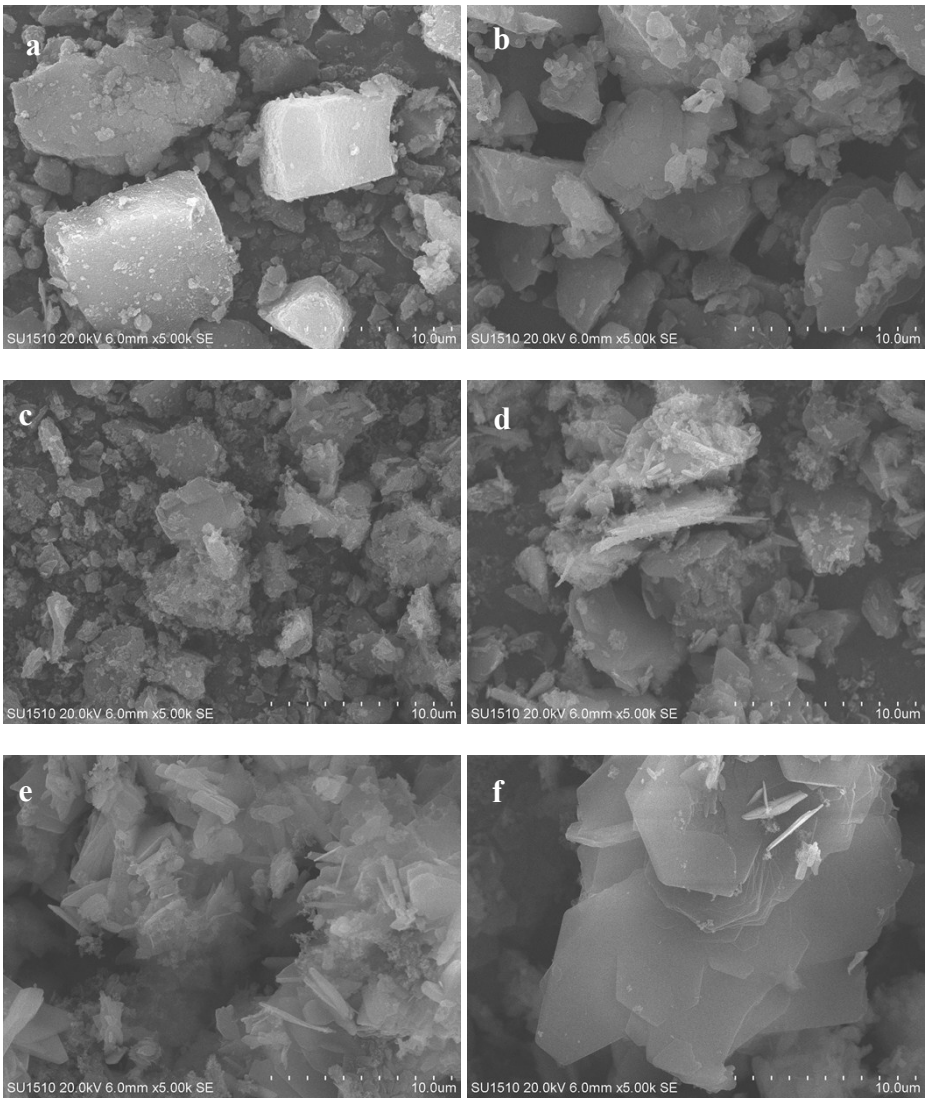

Fig. S6 SEM images of the S-RUB-36-180 crystallized at (a) 0, (b) 0.25, (c) 0.5, (d) 1.0, (e) 3.0, and (f) 4.0 days, respectively.

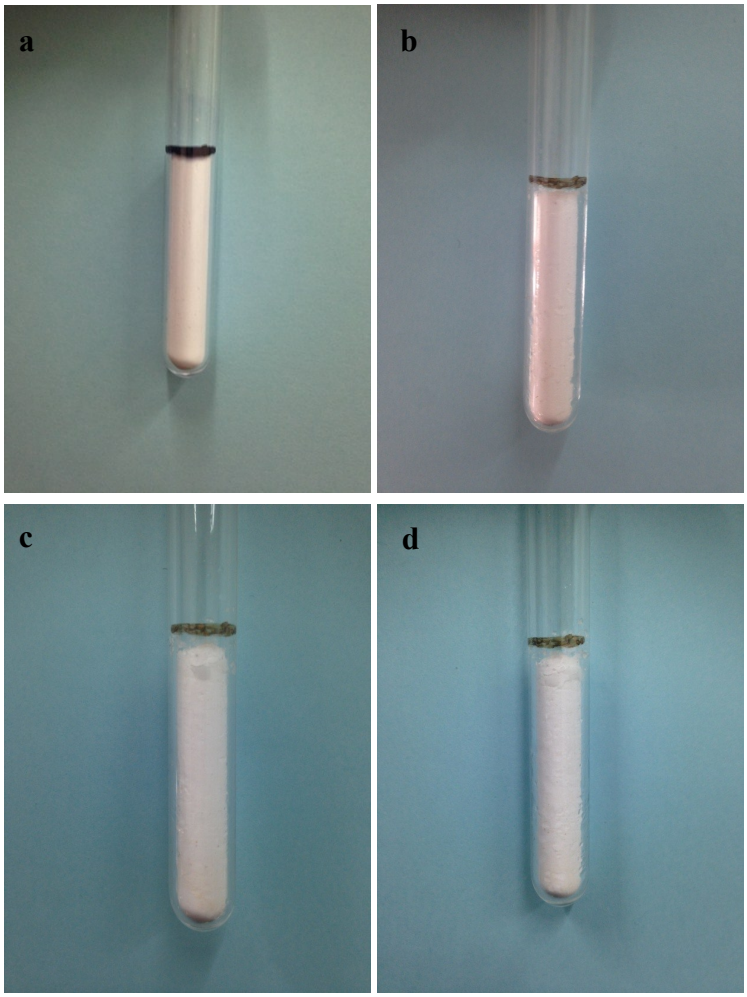

Fig. S7 Photographs of the S-RUB-36-180 crystallized at (a) 0, (b) 0.5, (c) 1.0, and (d) 4.0 days, respectively.

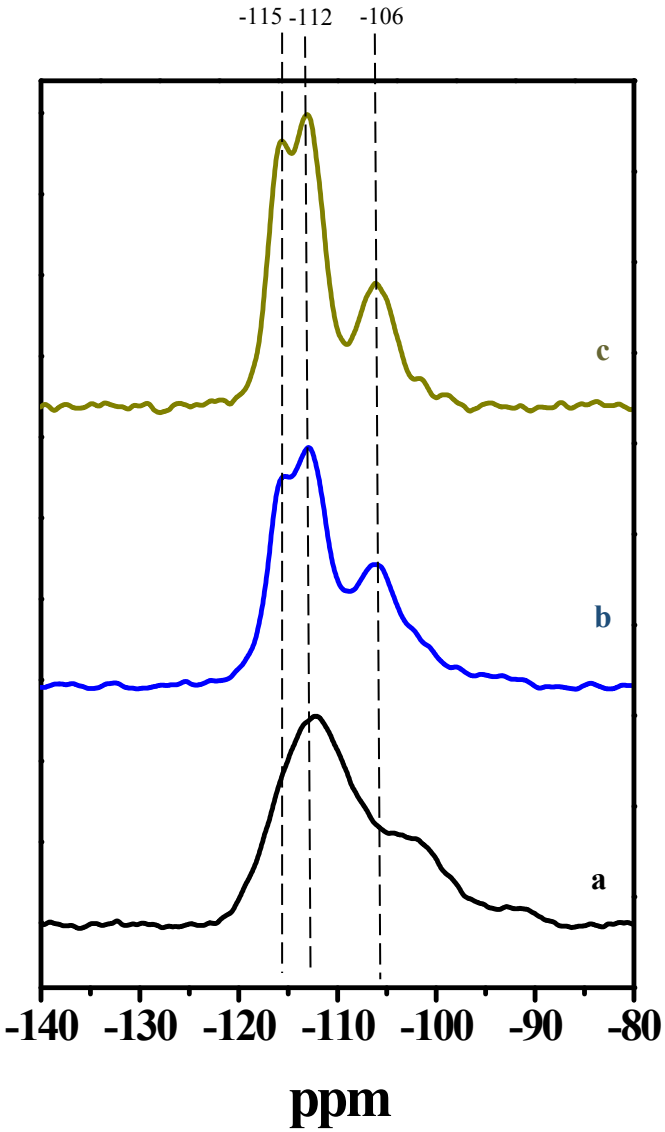

Fig. S8 ^{29}Si MAS NMR spectra of the S-RUB-36-180 crystallized at (a) 0, (b) 1.0, and (c) 4.0 days, respectively.

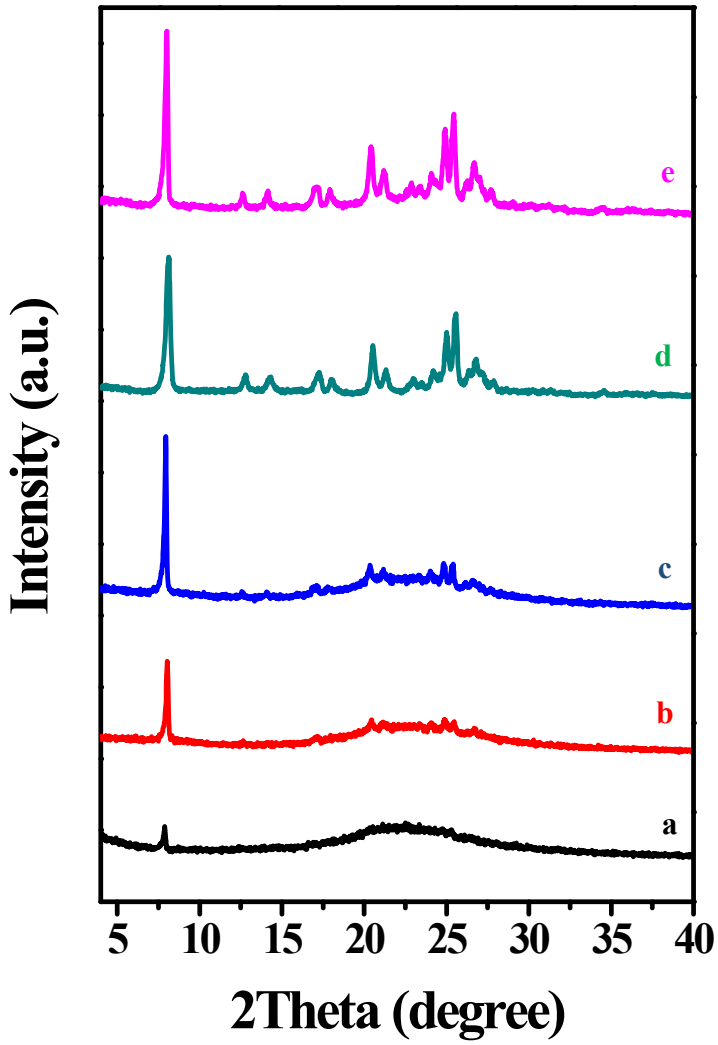

Fig. S9 XRD patterns of the S-RUB-36-140 crystallized at (a) 0, (b) 10, (c) 15, (d) 20, and (e) 25 days, respectively.

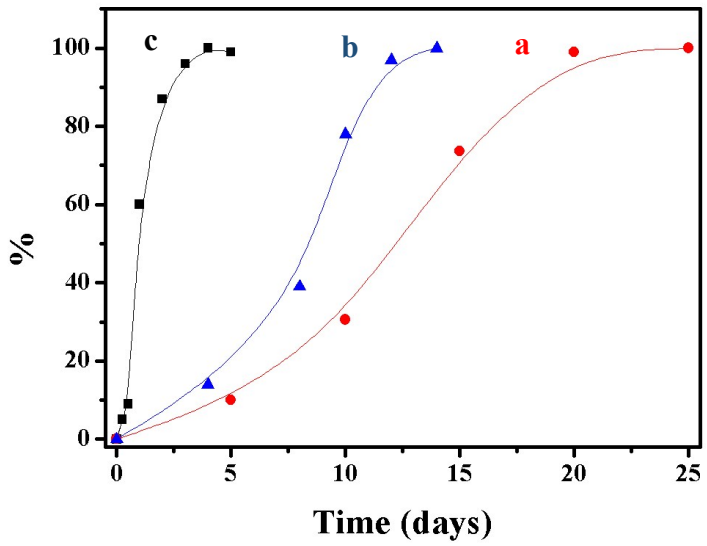

Fig. S10 The dependences of crystallinity on the crystallization time of the (a) C-RUB-36-140, (b) S-RUB-36-140, and (c) S-RUB-36-180.

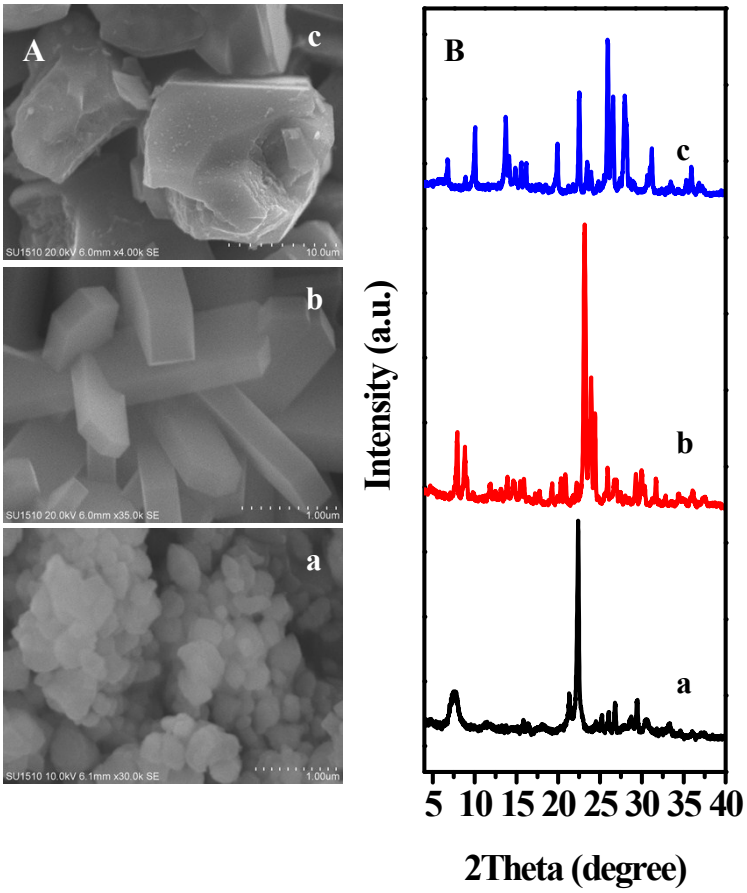

Fig. S11 (A) SEM images and (B) XRD patterns of the (a) Beta seeds, (b) MFI seeds, and (c) MOR seeds.

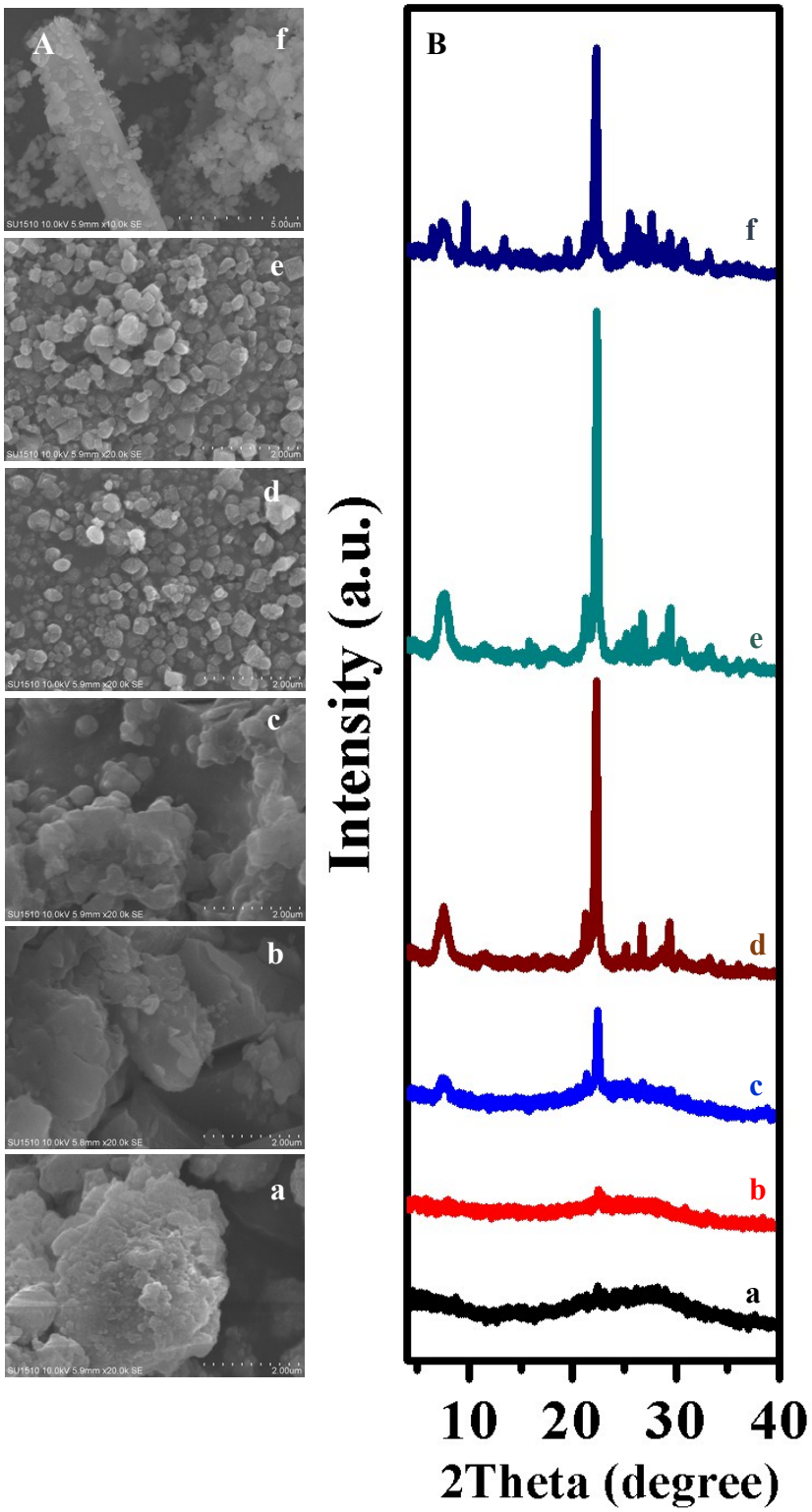

Fig. S12 (A) SEM images and (B) XRD patterns of the S-Beta-200 crystallized at (a) 0, (b) 0.5, (c) 1, (d) 1.5, (e) 4, and (f) 5 h, respectively. There is impurity of MOR zeolite when the crystallization time reaches to 5 h.

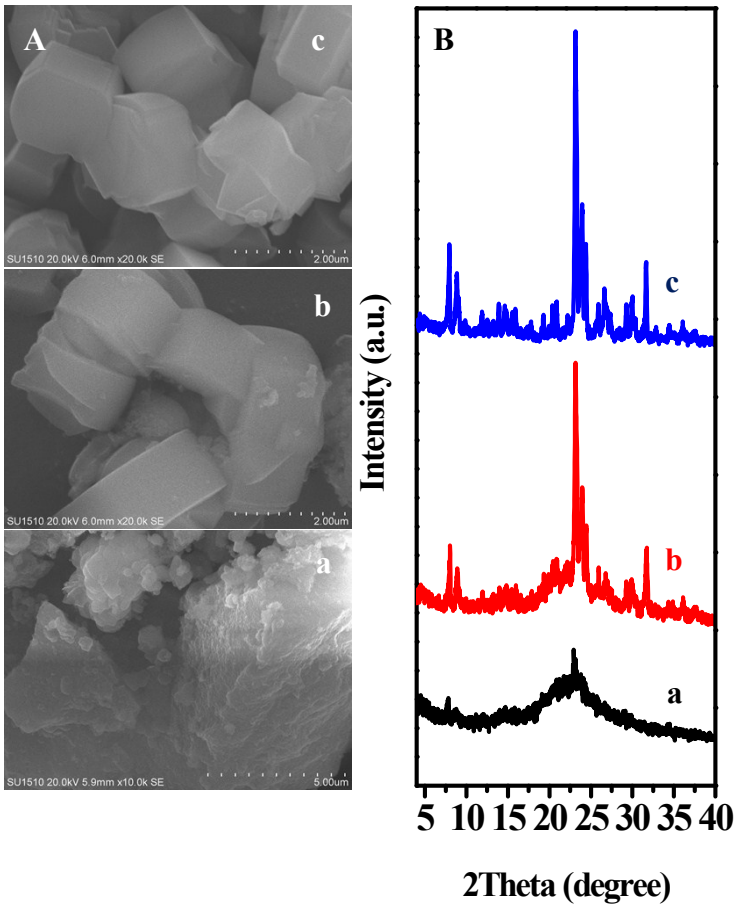

Fig. S13 (A) SEM images and (B) XRD patterns of the S-MFI-240 crystallized at (a) 0, (b) 0.35, and (c) 0.5 h, respectively.

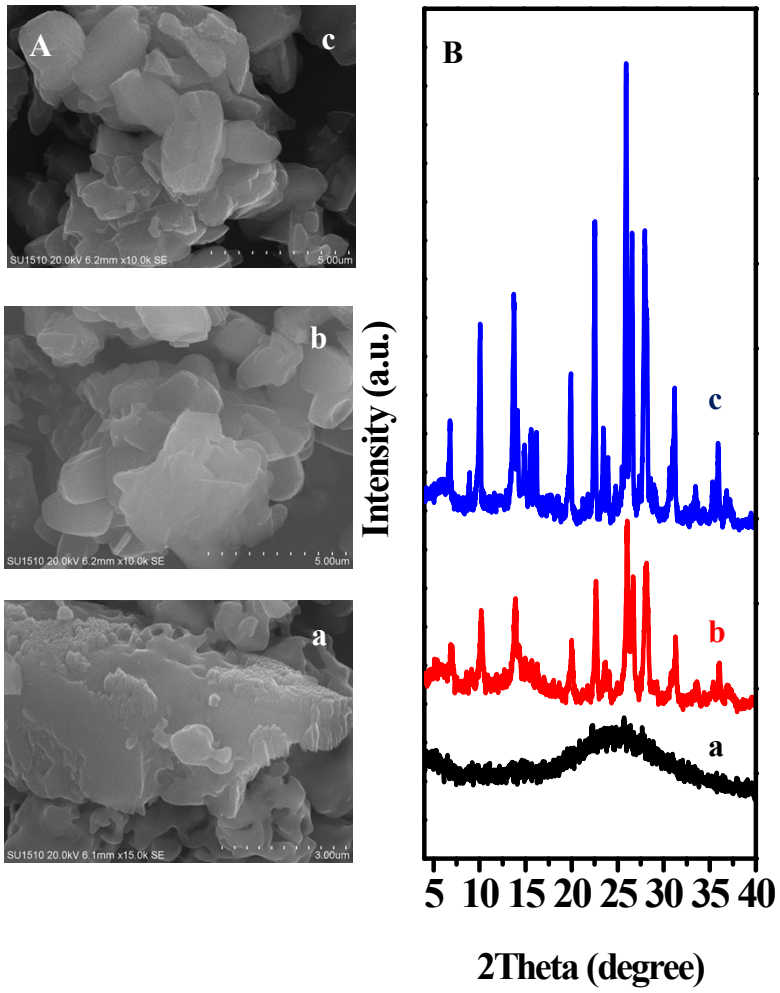

Fig. S14 (A) SEM images and (B) XRD patterns of the S-MOR-240 crystallized at (a) 0, (b) 1, and (c) 1.5 h, respectively.

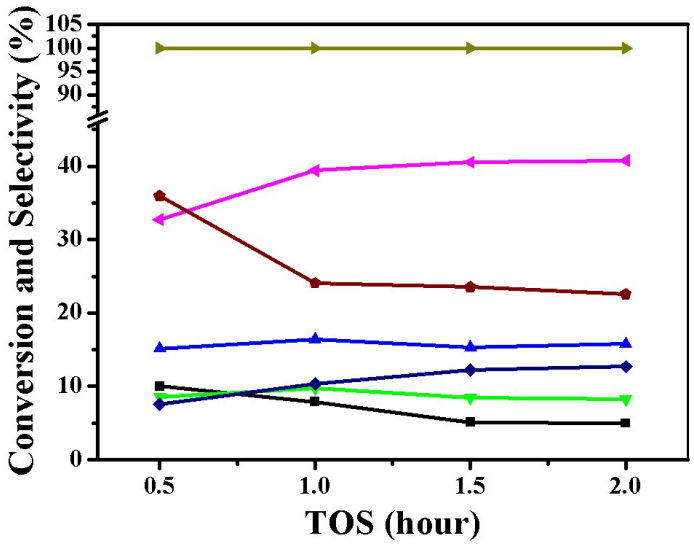

Fig. S15 Catalytic conversion and product selectivities over S-ZSM-5-240 catalyst in MTO (■ C_1; ▲$C_{2\text{-}4}$; ▼$C_2^=$; ◀$C_3^=$;◆$C_4^=$; ◷C_5+aromatics; ►Conv.).

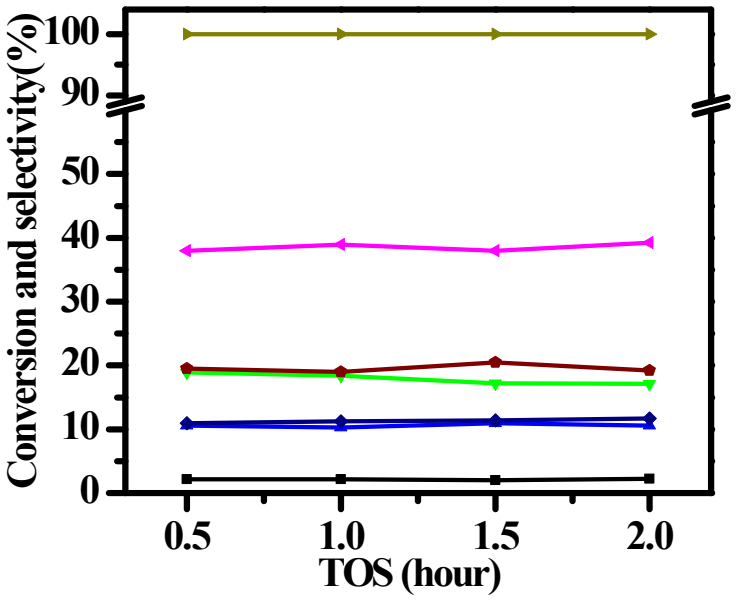

Fig. S16 Catalytic conversion and product selectivities over ZSM-5 catalyst by hydrothermal method at 180 °C in MTO (■ C_1; ▲C_{2-4}; ▼$C_2^=$; ◀$C_3^=$;◆$C_4^=$; ◷C_5+aromatics; ►Conv., the Si/Al ratio is 128 measured by ICP)